25th IMEKO TC4 International Symposium
23rd International Workshop on ADC and DAC Modelling and Testing
IMEKO TC-4 2022
Brescia, Italy / September 12-14, 2022

A novel CS-based measurement method for radial artery pulse wave estimation

Jozef Kromka[1], Jan Saliga[1], Ondrej Kovac[1], Luca De Vito[2], Francesco Picariello[2], Ioan Tudosa[2]

[1]*Technical University of Kosice, Letna 9, 04200 Kosice, Slovakia*
[1]*e-mail addresses: {jozef.kromka, jan.saliga, ondrej.kovac}@tuke.sk*
[2]*University of Sannio, Department of Engineering, 82100 Benevento, Italy*
[2]*e-mail addresses: {devito, fpicariello, ioan.tudosa}@unisannio.it*

***Abstract* – This paper presents a compressive sampling (CS) based measurement method for estimation of radial artery pulse wave from bio-impedance (Bio-Z) variation. The mathematical steps of the method, the 3D electrical model of the wrist used for simulations as well as the preliminary simulation investigations are presented. The reported result shows that the proposed method could be used to estimate radial artery pulse wave, which could be further used in blood pressure (BP) computation.**

I. INTRODUCTION

Measurement of hemodynamic parameters such as BP, heart rate (HR), and pulse transit time (PTT) plays a vital role in the prevention of cardiovascular diseases (CVD), which are the leading cause of death worldwide [1]. Continuous monitoring of hemodynamic parameters could improve the diagnosis and help in the early prevention of CVD [2], [3]. The methods for hemodynamic parameters measurement are relying on bulky and uncomfortable specific instruments, thus they are not suitable to carry out continuous monitoring [4]. Therefore, long-term monitoring of a patient should be carried out by means of a non-invasive method based on wearable instrumentation.

In literature, several non-invasive methods for hemodynamic parameters measurement have been proposed [5]. The methods relying on Bio-Z [6, 7] measurement appears to be the most promising for hemodynamic parameter measurement by wearables. In [8], the pulsation of blood inside the artery is measured by means of Bio-Z sensors. Therefore, by measuring arterial pulse on two points along the artery, PTT can be obtained and this could be used to estimate BP [9]. Bio-Z measurement system used for continuous BP monitoring was developed also in [10], where a single-channel impedance plethysmography measurement device was implemented. This device injects current with a frequency of 100 kHz to perform the measurement. Another recent published Bio-Z measurement system was presented in [7]. To perform the measurement, the developed device injects current with a frequency of 50 kHz. From literature survey, Bio-Z based measurement systems use as excitation signal a sine-wave at different frequencies [5]. This suggests that the optimal excitation frequency may change and depend on the patient. A broadband signal can be used instead of a sine-wave for estimating the radial artery pulse wave. In this case, a pulsed signal needs to be injected into the patient and then the obtained response acquired by an analog-to-digital converter (ADC). As broader is the frequency spectrum of the injected signal as higher should be the sampling frequency of the ADC. This limits the use of this technique for wearable device implementations, where low sampling frequency ADC are utilized to keep low the energy consumption and the amount of acquired data. In this paper, a CS method is proposed with the aim of reducing the sampling frequency of the ADC under the required Nyquist rate, thus overcoming the above mentioned limit. As a result, the radial artery pulse wave estimation from Bio-Z variation is obtained and afterwards it could be used for BP estimation.

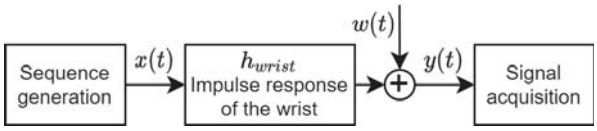

Fig. 1. The proposed measurement method.

The paper is organized as follows. In Section II, the mathematical formulation of the proposed method is presented. The preliminary experimental results obtained by means of simulation are reported in Section III. The main conclusion and some future work directions are drawn in Section IV.

II. THE PROPOSED METHOD

In this paper, the proposed measurement method is based on the determination of the impulse response of the radial artery on the wrist by exploiting a CS-based technique, followed by the estimation of the pulse wave propagation signal from the maximum values of the obtained impulse responses for each frame (i.e., time stamp).

The simplified block diagram of the proposed measurement method is shown in Fig. 1. This CS technique has its roots based on the DAC frequency response characterization method introduced in [11, 12]. Herein, in order to obtain the impulse response estimation of the wrist (i.e.,

$h_{wrist}(t)$), a pseudo-random binary sequence (PRBS) is used as an excitation signal. A finite number of input $x(n)$, with $n = 0, \ldots, N+L-1$ are considered for PRBS signal, where N and L are defined as follows: (i) $N \cdot T_u$ represents the duration of the acquisition window, and (ii) $L \cdot T_u$ is the maximum duration of the system impulse response, while T_u is the update interval of $x(n)$ samples. Let us model the $y(t)$ signal (see Fig. 1) as:

$$y(t) = x(t) * h_{wrist}(t) + w(t), \tag{1}$$

where $x(t)$ is defined as follows:

$$x(t) = \sum_{n=-L}^{N-1} x(n) \cdot \delta(t - nT_u). \tag{2}$$

In eq.(1), $w(t)$ is the additive white Gaussian noise (AWGN), which affects the $y(t)$, and in eq.(2), $\delta(t)$ is the Dirac's impulse function. Thus, the resulting $y(t)$ is further processed by an anti-aliasing filter and sampled by an ADC with sampling frequency f_{ADC}.

By defining $h_c(t) = h_{wrist}(t) * h_s(t)$, where $h_s(t)$ is the impulse response of the sampling system, the final impulse response $y_f(t)$ can be rewritten (i.e., cascade) as [12]:

$$\begin{aligned} y_f(t) &= x(t) * h_c(t) + w_f(t) = \\ &= \int_{-\infty}^{\infty} x(t-\tau) h_c(\tau) d\tau + w_f(t), \end{aligned} \tag{3}$$

where, $w_f(t) = w(t) * h_s(t)$. By taking into account eq.(2), while considering $h_c(t)$ as time invariant during the $x(n)$ generation, eq.(3) can be expressed as follows:

$$y_f(t) = \sum_{n=-L}^{N-1} x(n) \cdot h_c(t - nT_u) + w_f(t). \tag{4}$$

Eq.(4) can be discretized with a sampling period T_u, [12]:

$$\begin{aligned} &y_f(mT_u) = \\ &\sum_{n=-L}^{N-1} x(n) \cdot h_c[(m-n)T_u] + w_f(mT_u). \end{aligned} \tag{5}$$

In matrix form, it can be expressed as:

$$\mathbf{z} = \mathbf{X} \cdot \mathbf{h_c} + \mathbf{w_f}, \tag{6}$$

where $\mathbf{X}$ is represented as follows:

$$\mathbf{X} = \begin{bmatrix} x(0) & x(-1) & \cdots & x(-L+1) \\ x(1) & x(0) & \cdots & x(-L) \\ \vdots & \vdots & \ddots & \vdots \\ x(N-1) & x(N-2) & \cdots & x(N-L-2) \end{bmatrix}, \tag{7}$$

and $\mathbf{z}$, $\mathbf{w_f}$ and $\mathbf{h_c}$ are written as:

$$\begin{aligned} \mathbf{z} &= [y_f(0), y_f(T_u), \ldots, y_f((N-1)T_u)]^T \\ \mathbf{w_f} &= [w_f(0), w_f(T_u), \ldots, w_f((N-1)T_u)]^T. \\ \mathbf{h_c} &= [h_c(0), h_c(T_u), \ldots, h_c((N-1)T_u)]^T \end{aligned} \tag{8}$$

The sampled version of the system impulse response is considered K-sparse in the time domain, considering that it contains K non-zero coefficients, where $K < L$. To exploit the sparsity of the system impulse response in the time domain, the ADC can work at a sampling frequency lower than the Nyquist frequency $f_u = 1/T_u$. By using a much lower sampling frequency, during the time window $N \cdot T_u$, the ADC will acquire only M samples, $m = 0, ...M-1$, expressed as $y(m) = [y(1), y(2), \ldots, y(M-1)]^T$. Here, the downsampling factor represents the compression ratio, $CR = f_u/f_{ADC}$. This operation can be modeled as follows:

$$\mathbf{y} = \mathbf{R} \cdot \mathbf{X} \cdot \mathbf{h_c} + \mathbf{w_f}. \tag{9}$$

In eq.(9), $\mathbf{R}$ is a $M \times N$ matrix, which represents the downsampling process by CR factor. If $M < L$ in the time domain, then $\mathbf{h_c}$ can be estimated by solving the following minimization problem:

$$\begin{aligned} \widehat{\mathbf{h_c}} &= arg \min_{\mathbf{h_c}} ||\mathbf{h_c}||_1 \\ subject\ to &: \mathbf{y} = \mathbf{R}\mathbf{X}\mathbf{h_c}, \end{aligned} \tag{10}$$

where $|| \cdot ||_1$ represents the l_1 norm operator. A solution to the problem in eq.(10) can be obtained by using various algorithms [13]. However, in this study, the orthogonal matching pursuit (OMP) algorithm was used [14].

According to [7], the impedance of the radial artery changes with the the radial artery area. Therefore, in present study, the impedance change that would cause a proportional change in the impulse response was assumed. In consequence, the pulse wave propagation signal $x_t[n]$ is obtained from the maximum values of the obtained impulse responses for each frame duration.Thus, $\widehat{x}_t[n]$ is obtained from maximum values of $\widehat{h}_{wrist}(t)$.

III. SIMULATION ANALYSIS

A. *The 3D electrical model of the wrist*

In this work, a modified version of the wrist 3D electrical model described in [15] was considered. To this aim, two different datasets were considered. The first dataset [16] was used to define the electrical impedance of tissues. This dataset contains dielectric properties of several biological tissues from frequency $f = [10\,\text{Hz} - 100\,\text{GHz}]$. The second dataset [17] was used to model blood flow inside the radial artery. This dataset contains blood pressure, blood flow speed, and artery area values for different arteries.

The developed model consists of 3D impedance voxels as shown in Fig. 2. This impedance voxel is a cube made of

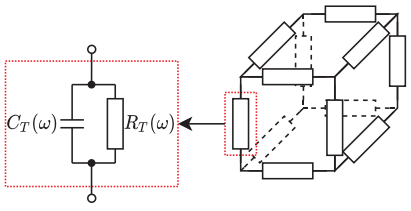

Fig. 2. The equivalent electrical circuit of the voxel.

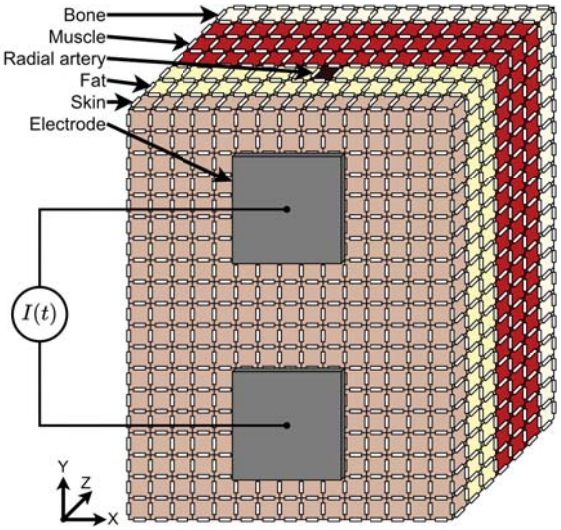

Fig. 3. The developed 3D wrist model.

parallel combinations of resistance and capacitance values. The resistance $R_T(\omega)$ and capacitance $C_T(\omega)$ are calculated as follows. First, the complex permittivity is obtained for the required frequency from the dataset in [16]. Then impedance is calculated by the following formula [18]:

$$Z_T(\omega) = \frac{1}{j\omega C_0 \varepsilon_T^*(\omega)}, \tag{11}$$

where $\omega = 2\pi f$, $\varepsilon_T^*(\omega)$ is the complex permittivity of tissue and $C_0 = \frac{A\varepsilon_0}{d}$, with A is the area of the tissue, d is the depth, and ε_0 is the permittivity of vacuum. Since the model is created by cube voxels, thus $A = d \cdot d$, then the eq.(11) can be simplified as:

$$Z_T(\omega) = \frac{1}{j\omega d \varepsilon_0 \varepsilon_T^*(\omega)}. \tag{12}$$

$R_T(\omega)$ and $C_T(\omega)$ are calculated from $Z_T(\omega)$ as follows:

$$R_T(\omega) = \frac{1}{\mathbf{Re}\left(\frac{1}{Z_T(\omega)}\right)}, \; C_T(\omega) = \frac{\mathbf{Im}\left(\frac{1}{Z_T(\omega)}\right)}{\omega}. \tag{13}$$

The impedance voxels with their respective values are then connected in a 3D configuration, thus forming the 3D wrist electrical model (see Fig. 3). The size of the voxel edge (i.e., d) was set to 2 mm, and the used type of tissues are skin, fat, blood, muscles, and bone. The total size of the 3D wrist model is 30×38×14 mm, where: (i) the first layer is the skin layer, (ii) the second and third layers are fat, (iii) a radial artery which is located around 2 mm inside the fat layer under the skin [19], (iv) three layers are the muscle layer, and (v) the bottom layer which is modeled as a bone. The Bio-Z sensing electrodes have size of 10×10 mm and are placed on top of the skin, positioned 10 mm from each other, with radial artery in the middle, below the electrodes.

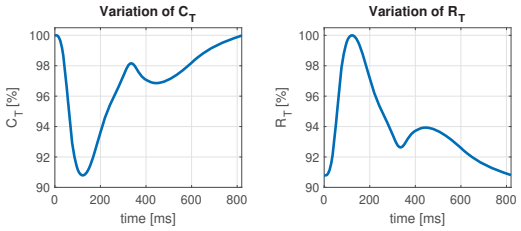

Fig. 4. Percentage variation of R_T and C_T in time.

In order to simulate the blood flow inside the radial artery, the dataset of the first subject (which consists of 411 points sampled at 500 Hz) in [17] was used to evaluate how the capacitance and resistance were changing (i.e., the area data were used in eqs.(11) and (13)). From the simulation results, a variation about 10 % for capacitance and resistance of the radial artery was obtained (e.g., proportionally to the area of the radial artery R_T was increasing while C_T was decreasing).

Thus, the obtained time variations shown in Fig. 4 were used to model radial artery voxels during blood flow. In these voxels, the values of capacitance and resistance were changed according to their variation at an imposed time stamp of 2 ms. For example, the next voxel along the y-axis, has its own variation for the successively time stamp that is considered, and so on.

The netlist of the 3D wrist electrical model was generated by using MATLAB, while the simulation was performed by means of LTspice. Since there are different values of resistance and capacitance with the frequency variation, the model was made in a way that for each frequency, a new netlist is generated and then it is simulated by using AC analysis. In order to obtain the impedance value, a current source of 500 μA was used as shown in Fig. 3, while the voltage on the electrodes was read and the complex impedance was calculated.

In order to simulate the proposed CS-based measurement method, a local dataset was generated using the previously described 3D wrist electrical model, consisting of 411 frequency responses of the wrist impedance. Each frequency response represents the state of the wrist at 411 time stamps (i.e., each of 2 ms) according to blood flow inside the radial artery. The frequency responses are recorded for over 500 different frequency points linearly distributed from 10 Hz to 1 GHz.

B. Simulation setup

In Fig. 5, a simplified circuit model describing the adopted simulation setup is depicted. Herein, R_i is a resistor used to reduce the injected current into the body and to measure the output signal $y(t)$, $Z_{wrist}(\omega)$ is the impedance of the wrist generated by the 3D wrist electrical model. The output signal $y(t)$ is obtained by calculating the current flow according to the Ohm's law, by obtaining the

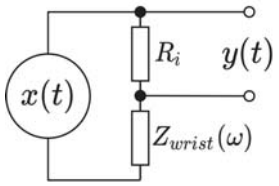

Fig. 5. Simplified simulation circuit.

impedance change of the wrist $Z_{wrist}(\omega)$ depending on the $x(t)$ frequency, and by applying the fast Fourier transform (FFT) of the voltage-frequency spectrum of $x(t)$. Furthermore, by using inverse FFT, the current flow in the time domain is evaluated. This current is then multiplied by the resistance R_i and thus, the output signal $y(t)$ is obtained. Since the developed dataset contains a discretized version of the frequency response different from the simulated one, the dataset was interpolated to estimate the missing frequencies components needed for the simulations.

In particular, the discrete time processing steps are summarized in the following. The $x[n]$ signal (e.g., PRBS sequence) is generated having a length of $N + L$ samples. Then the sequence is used to generate $x(t)$ by simulating the output of a digital-to-analog converter (DAC) working at a simulation frequency f_{sim}. The DAC's output is modelled to update the samples of $x[n]$ at T_u with n_{DAC} resolution, FS_{DAC} full-scale and SNR_{DAC} as signal to noise ratio (SNR). In the simulation, the low-pass filtering of $x(n)$ with the order of filter $Nord_{DAC}$ and with the cut-off frequency fl_{DAC} was also considered. Then $x(t)$ was used to stimulate the $h_{wrist}(t)$ thus to obtain $y(t)$ according to the proposed method (see Fig. 5).

The acquisition of $y(t)$ was realized by simulating: (i) an ADC having $f_{ADC} = f_u/CR$ sampling frequency, n_{ADC} bit resolution, and FS_{ADC} full scale input voltage, and (ii) an anti-aliasing filter having $Nord_{ADC}$ the order and fl_{ADC} cutoff frequency. In Table 1, all the values of the above listed parameters are given.

The proposed CS-based method was then evaluated for different CR in terms of root mean square error $RMSE$ as main figure of merit. The $RMSE$ was calculated from the magnitude of the CS-based estimated impulse response $\widehat{H}(k/T_u)$, respect to the actual impulse response, $H(k/T_u)$ as:

$$RMSE\big|_{dB} = \sqrt{\frac{1}{L}\sum_{k=0}^{L-1}\left[|\widehat{H}(k)|_{dB} - |H(k)|_{dB}\right]^2}. \quad (14)$$

Furthermore, Monte Carlo analyses have been performed on 100 trials, always with a different $x[n]$, and the resulting $RMSE$ values were averaged and expressed as $RMSE_m$.

The reconstruction quality of the pulse wave propagation signal inside the radial artery was evaluated in terms of

Table 1. Parameters used for simulation.

f_{sim}	8 MHz
f_{update}	1 MHz
n_{DAC}	12 bit
FS_{DAC}	2 V
SNR_{DAC}	70 dB
$Nord_{DAC}$	100
fl_{DAC}	1.2 MHz
R_i	500 Ω
CR	2, 4, 8, 16
N	1024
L	1024, 512, 256, 128
n_{ADC}	16 bit
FS_{ADC}	2 V
$Nord_{ADC}$	2000
fl_{ADC}	0.45 MHz

percentage root mean squared difference PRD [13]:

$$PRD = \sum_{n=1}^{N} \frac{||x_t[n] - \widehat{x}_t[n]||_2}{||x_t[n]||_2} \cdot 100[\%], \quad (15)$$

where, $x_t[n]$ is ideal pulse wave propagation signal, $\widehat{x}_t[n]$ is reconstructed pulse wave propagation signal, and $||\cdot||_2$ represents the l_2 norm operator.

C. Preliminary results

The first performed simulation test was focused to observe how CR affects on the reconstruction quality of each $\widehat{h}_{wrist}(t)$. The results for the considered CR and L values reported in Table 1 are shown in Fig. 6, where the $RMSE_m$ values were plotted as red dots, and the maximum and the minimum values as blue bars.

The next evaluated simulation test was concentrated to observe the influence of L length on the reconstruction quality of each $\widehat{h}_{wrist}(t)$, by considering three different CR values and various L lengths. In Fig. 7, the $RMSEm$ variation for $CR = 2$ is shown, for values of L changing from 576 to 1024 with step of 64, where it can be observed that there is no significant changes in $RMSEm$ variation up to $L = 768$.

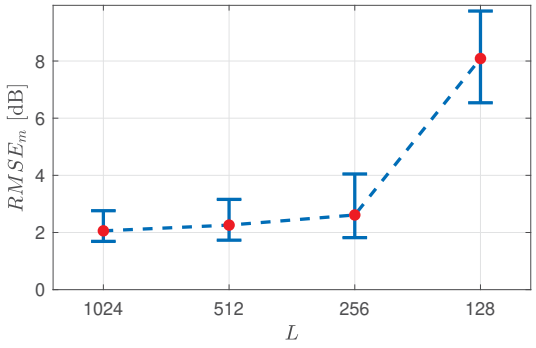

Fig. 6. $RMSE_m$ variation against CR and L.

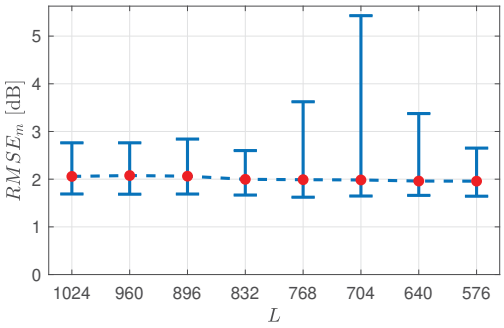

Fig. 7. $RMSE_m$ variation with $CR = 2$ against L.

In Fig. 8, the obtained $RMSEm$ variations for $CR = 4$ are shown, by considering L changing from 320 to 1024 with step of 64. Similarly, as in the previous case, there is no significant changes in $RMSEm$ variation up to $L = 320$.

At the end of the second experiment, $RMSEm$ results for $CR = 8$ were evaluated. The results are shown in Fig. 9. The simulation was performed for L from 192 to 1024 with step of 64.

In this case, $RMSEm$ changes against the number of the adopted L. In particular, the $RMSE$ averages slightly decrease with the increasing of L. From 320 the average started to rise again, but the minimum values were still declining. The best $RMSE$ was obtained for $L = 192$. The results below 192 are not shown because the method could not reconstruct the impulse response with a lower number of L.

The last performed simulation analysis was carried out with the aim to observe the variation of the $\widehat{x}_t[n]$ respect to $x_t[n]$. Because of the reconstruction error, the blood propagation wave contains a high amount of high-frequency noise. Therefore the obtained results were filtered with a filter with cutoff frequency of 10 Hz. Three different simulations were performed for $CR = 2, 4, 8$. The results are shown in Fig. 10.

The value of PRD was calculated for the reconstructed $\widehat{x}_t[n]$ according to the reference pulse wave $x_t[n]$ signal (i.e., actual, obtained without using CS) shown in Fig. 10 a). Thus, for the case b) where $CR = 8$, $PRD = 11.668\%$ was obtained, for case c) with $CR = 4$, $PRD = 10.720\%$,

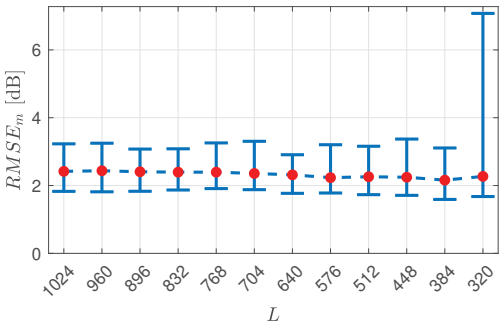

Fig. 8. $RMSE_m$ variation with $CR = 4$ against L.

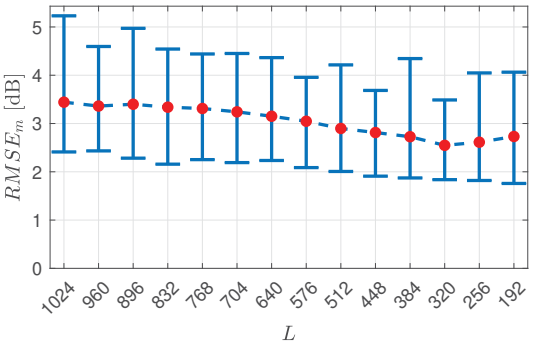

Fig. 9. $RMSE_m$ variation with $CR = 8$ against the L.

while for case d) where the $CR = 2$ the $PRD = 7.954\%$ was obtained. In all cases, the estimated and reconstructed pulse wave propagation signal can be utilized to calculate PTT in a further processing step. Consequently, in order to compute PTT, data coming from two pulse wave propagation signals of the blood circulating for radial artery are needed together with their known distance. In this case, the same proposed measurement method could be used with two additional Bio-Z electrodes placed to a known distance.

IV. CONCLUSION AND FUTURE WORK

In this paper, a novel measurement method using CS for estimating the pulse wave propagation which can be used as a non-invasive technique for BP assessment was presented. The method exploits the time domain sparsity of the impulse response of the wrist. As it was expected, the proposed measurement method based on CS could be utilized to develop a BP sensing system. The obtained simulation results confirmed that the impulse response of the

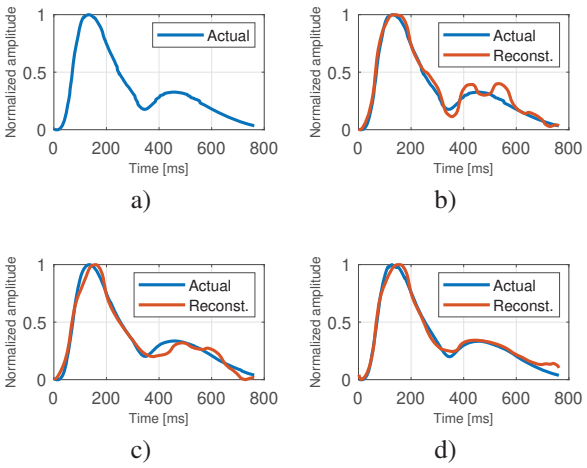

Fig. 10. a) actual pulse wave propagation, b) reconstruction of pulse wave propagation with $CR = 8, L = 320$, $PRD = 11.668\%$, c) reconstruction of pulse wave propagation with $CR = 4, L = 384$, $PRD = 10.720\%$, d) reconstruction of pulse wave propagation with $CR = 2, L = 640$, $PRD = 7.954\%$.

wrist is changing according to the change in blood flow area inside the radial artery. The simulations also proved that the proposed CS-based measurement method is able to sense this change in the impulse response.

Further work is directed to: (i) implement a hardware prototype, (ii) improve the simulation model, (iii) search for optimal configuration parameters for the proposed measurement method in order to maximize the reconstruction quality of the pulse wave, and (iv) assess the comparison of the experimental results with the results obtained in simulations.

ACKNOWLEDGMENT

The work is a part of the project supported by the Science Grant Agency of the Slovak Republic (No. 1/0413/22).

REFERENCES

[1] R. Jagannathan, S. A. Patel, M. K. Ali, and K. Narayan, "Global updates on cardiovascular disease mortality trends and attribution of traditional risk factors," *Current diabetes reports*, vol. 19, no. 7, pp. 1–12, 2019.

[2] G. Parati, G. S. Stergiou, E. Dolan, and G. Bilo, "Blood pressure variability: clinical relevance and application," *The Journal of Clinical Hypertension*, vol. 20, no. 7, pp. 1133–1137, 2018.

[3] M. H. Mehlum, K. Liestøl, S. E. Kjeldsen, S. Julius, T. A. Hua, P. M. Rothwell, G. Mancia, G. Parati, M. A. Weber, and E. Berge, "Blood pressure variability and risk of cardiovascular events and death in patients with hypertension and different baseline risks," *European heart journal*, vol. 39, no. 24, pp. 2243–2251, 2018.

[4] A. Barszczyk and K. Lee, "Measuring blood pressure: from cuff to smartphone," *Current Hypertension Reports*, vol. 21, no. 11, pp. 1–4, 2019.

[5] T. Panula, J.-P. Sirkia, D. Wong, and M. Kaisti, "Advances in non-invasive blood pressure measurement techniques," *IEEE Reviews in Biomedical Engineering*, pp. 1–1, 2022.

[6] S. Grimnes and O. G. Martinsen, *Bioimpedance and bioelectricity basics*. Academic press, 2011.

[7] T.-W. Wang, W.-X. Chen, H.-W. Chu, and S.-F. Lin, "Single-channel bioimpedance measurement for wearable continuous blood pressure monitoring," *IEEE Transactions on Instrumentation and Measurement*, vol. 70, pp. 1–9, 2021.

[8] R. Mukkamala, J.-O. Hahn, O. T. Inan, L. K. Mestha, C.-S. Kim, H. Töreyin, and S. Kyal, "Toward ubiquitous blood pressure monitoring via pulse transit time: Theory and practice," *IEEE Transactions on Biomedical Engineering*, vol. 62, no. 8, pp. 1879–1901, 2015.

[9] C. Poon and Y. Zhang, "Cuff-less and noninvasive measurements of arterial blood pressure by pulse transit time," in *2005 IEEE Engineering in Medicine and Biology 27th Annual Conference*, pp. 5877–5880, 2005.

[10] T. H. Huynh, R. Jafari, and W.-Y. Chung, "Noninvasive cuffless blood pressure estimation using pulse transit time and impedance plethysmography," *IEEE Transactions on Biomedical Engineering*, vol. 66, no. 4, pp. 967–976, 2018.

[11] L. De Vito, F. Picariello, and I. Tudosa, "A novel measurement method for dac frequency response characterization," in *24th IMEKO TC4 International Symposium and 22nd International Workshop on ADC and DAC Modelling and Testing, IWADC 2020*, pp. 395–400, International Measurement Confederation (IMEKO), 2020.

[12] L. De Vito, F. Picariello, S. Rapuano, and I. Tudosa, "A new built-in loopback test method for digital-to-analog converter frequency response characterization," *Measurement*, vol. 182, p. 109712, 2021.

[13] J. Šaliga, I. Andráš, P. Dolinskỳ, L. Michaeli, O. Kováč, and J. Kromka, "Ecg compressed sensing method with high compression ratio and dynamic model reconstruction," *Measurement*, vol. 183, p. 109803, 2021.

[14] J. A. Tropp and A. C. Gilbert, "Signal recovery from random measurements via orthogonal matching pursuit," *IEEE Transactions on information theory*, vol. 53, no. 12, pp. 4655–4666, 2007.

[15] B. Ibrahim, D. A. Hall, and R. Jafari, "Pulse wave modeling using bio-impedance simulation platform based on a 3d time-varying circuit model," *IEEE Transactions on Biomedical Circuits and Systems*, vol. 15, no. 1, pp. 143–158, 2021.

[16] S. Gabriel, R. W. Lau, and C. Gabriel, "The dielectric properties of biological tissues: III. parametric models for the dielectric spectrum of tissues," *Physics in Medicine and Biology*, vol. 41, pp. 2271–2293, nov 1996.

[17] P. H. Charlton, J. Mariscal Harana, S. Vennin, Y. Li, P. Chowienczyk, and J. Alastruey, "Modeling arterial pulse waves in healthy aging: a database for in silico evaluation of hemodynamics and pulse wave indexes," *American Journal of Physiology-Heart and Circulatory Physiology*, vol. 317, no. 5, pp. H1062–H1085, 2019. PMID: 31442381.

[18] J. R. Macdonald and E. Barsoukov, *Impedance spectroscopy: theory, experiment, and applications*. John Wiley & Sons, 2018.

[19] J. U. Kim, Y. J. Lee, J. Lee, and J. Y. Kim, "Differences in the properties of the radial artery between cun, guan, chi, and nearby segments using ultrasonographic imaging: a pilot study on arterial depth, diameter, and blood flow," *Evidence-Based Complementary and Alternative Medicine*, vol. 2015, 2015.